TECHNICAL PAPER

CrossMark

A novel numerical modeling paradigm for bio particle tracing in non-inertial microfluidics devices

Amirali Ebadi[1] · Reihaneh Toutouni[2,3] · Mohammad Javad Farshchi Heydari[5] · Morteza Fathipour[1,2] ·
Madjid Soltani[4,5]

Abstract
In this work, we report on the design and implementation of a new method for the two dimensional (2D) simulation of rigid spherical particles trajectory which are to be separated in a microfluidics device based on their sizes. The advantages of efficient particle trajectory simulation method (EPTSM) include drastically smaller runtimes as compared with other methods as well as the ability to include particle collisions with channel's walls and its ability to be extended to 3D simulations. Numerically simulated results were verified using a specifically designed and fabricated deterministic lateral displacement microfluidic device test structure. The method has provided realistic results for the study of multi-particles throughout the entire channel.

1 Introduction

Bio particle separation, is an emerging technology with important applications in areas such as separation and detection of rare cells, although some target particles have extremely low concentration in the blood, they play an important role in medical diagnosis and treatment Bio particle separation is often the first stage in bioparticle analysis. The microfluidics approach is one of the most desirable methods for particle separation (Smith et al. 2012). Several methods are used in this field, these include dielectrophoresis (Çetin and Li 2011), affinity-based (Hyun and Jung 2013), hydrophoresis (Choi et al. 2014) and

magnetophoresis (Krishnan et al. 2009). Each method is based on a specific physical behavior of the particles, e.g. charge, mass, size and the magnetic moment. These methods may also be divided into "label free" and "marker-based" categories. Label-free separation procedures have several advantage over marker-based methods, including lower cost, less damage to the particle under test and simplicity.

Deterministic lateral displacement (DLD) devices are microfluidics devices used to separate particles according to their sizes. DLD has provided the highest resolution among the microfluidics separators (Huang et al. 2004). Furthermore, it induces a small shear stress on the particles; thus enjoys suitable criteria for bio particle separation with different sizes (Huang et al. 2004; Vig 2010; Balvin et al. 2009; Inglis et al. 2006; Beech et al. 2009; Beech 2005; Zheng 2005; Davis et al. 2006). These devices are made of rows of micro pillars arranged such that each row is shifted by a certain distance across the channel with the one next to it. Optimal efficiency in these devices is achieved when they are operated in the laminar flow regime. Under such circumstances, particles follow within the fluid streamlines until they clash with the micro pillars or walls. While the streamline containing the particle passes through the space between two pillars, the particle may collide with a pillar. If the distance between the center of the particle and the nearest pillar is less than the particle radius, particles move along the streamlines, zigzagging

✉ Morteza Fathipour
mfathi@ut.ac.ir

1 MEMS and NEMS Laboratory, Department of Electrical and Computer Engineering, Faculty of Engineering, University of Tehran, Tehran, Iran

2 Device Simulation and Modeling Laboratory, Department of Electrical and Computer Engineering, Faculty of Engineering, University of Tehran, Tehran, Iran

3 Department of Petroleum Engineering, University of Wyoming, Laramie, WY, USA

4 Centre for Biotechnology and Bioengineering (CBB), University of Waterloo, Waterloo, ON, Canada

5 Department of Mechanical Engineering, K. N. Toosi University of Technology, Tehran, Iran

through the gaps between pillars. If the particles are smaller than a certain "critical diameter" (determined by the DLD device geometry), the net lateral displacement of the particle at the end of the channel is approximately zero. On the other hand, if particles are larger than the critical diameter, they move into new streamlines with upward direction. Under this situation, the particles cannot pass through the inter-pillar gaps and will bump into the pillars that are located with a positive incline so the particles move upward. The geometry of the micro pillar array determines the net lateral displacement of particles at the end of the channel (Chen et al. 2014; Jin et al. 2014; McGrath et al. 2014; Beech 2011).

Hence, when a mixture of particles with different sizes is being used as the inflow of the DLD, the larger particles will be laterally displaced while the smaller particles will move in streamlines with no net lateral displacement. Consequently, the DLD device can be employed as a desirable separator device and can sort particles according to their sizes and deformability (Quek et al. 2011). Applications of this device include the separation of palates, RBC and WBC from whole blood (Davis et al. 2006), enrichment of cells for tissue engineering (Green et al. 2009) determination of cell size (Inglis et al. 2008), separation of rare cells (Quek et al. 2011), etc.

Numerical Simulation tool is a valuable means for the identification of optimal design for microfluidics devices. Krüger et al. (2014) performed three-dimensional immersed-boundary finite-element Lattice–Boltzmann simulations for finding trajectory of a deformable particle in a part of a DLD device. Quek et al. (2011) studied the separation of deformable bodies in DLD using numerical simulations that relied on the immersed boundary method in a two dimensional model. Their simulation used periodic top and bottom boundaries, although such boundary conditions may not be encountered in realistic DLD devices since channel's width is finite. Al-Fandi et al. (2011) performed a two dimensional simulation of a rigid particle trajectory in a DLD device. However, neglecting wall effects resulted in an inaccurate simulation that lacked the functionality of a real DLD device.

In this presented paper, the bio-particles trajectories simulation in a microchannel is approached by a whole different perspective which reduces simulation load and time in a noticeable manner. This approach is named efficient particle trajectory simulation method (EPTSM) by the authors. To elaborate what we have done, the velocity profile of the fluid in each position of the channel is obtained by conventional finite element method simulation of the microchannel and is used for tracking the bioparticles trajectory by proposed method which is briefly explained in Fig. 2 flowchart. The particle position in each time step is calculated based on the information of its last

position, fluid velocity field and its collision with channel's walls. EPTSM allows to realistically simulate the whole device for several particles while including the wall-particle interactions through the channel. As pillars are repeated in large enough numbers, particle–particle interaction does not hinder the separation process and further collisions with pillars completes separation process. Therefore, within frame work of the DLD theory one can safely neglect particle–particle interactions. Thus we neglect such interactions.

To validate these simulation results, polystyrene (PS) beads in different sizes were employed. Experimental data shows that particle trajectories of polystyrene beads closely tracked those simulation results predicted. The details of this method is discussed in the next section.

2 Materials and methods

2.1 The DLD theory

Deterministic lateral displacement (DLD) device consists of micro pillars that are arranged periodically, with a center to center distance between the nearest pillars in each row of λ and the slope ε, as shown in Fig. 1a. So the shift between pillars in two subsequent rows is $\varepsilon\lambda$. The DLD device consists of several periods of pillar sets in series. Number of pillars in a row along a set is $n = 1/\varepsilon$, where n is an integer. Therefore, the total amount of fluid flux through each two adjacent pillars is divided by n flow streams. The first flow stream width is called β. If the particle radius is smaller than the first flow stream, it remains in that flow stream. Typically, this mode of operation is referred to as "ZigZag mode". But if the particle diameter is larger than the critical size $D_c = 2\beta$, it cannot continue its path between pillars and moves to a second flow stream. The same pattern occurs as the particle collides with subsequent pillars. Thus, particles with larger diameters follow the alternative streamlines, and this mode of operation is called "bump mode". As a result, the DLD separates larger particles from smaller ones.

The width of the first stream flow can be calculated by integration of the flow profile u(x) as follows:

$$\int_0^\beta u(x)dx = \varepsilon \int_0^g u(x)dx \qquad (1)$$

where, g is the gap between pillars. In creeping flow regime with Reynolds number less than 1, one can assume the flow profile to be parabolic with no-slip boundary condition near the pillar walls. Therefore, the flow profile can be written as:

Fig. 1 Schematics of a DLD device: **a** a segment of DLD device, showing essential geometry. **b** Fluid streamlines passing through two adjacent pillars. **c** Motion of particles in zigzag and bump mode. Additionally, β which is first flow stream width and equals $D_c/2$ is shown
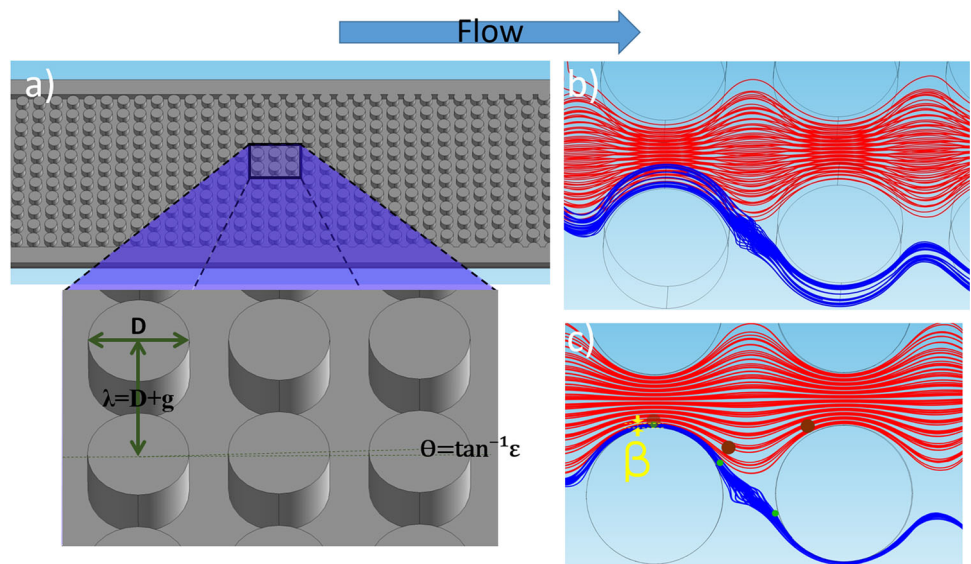
$$u(x) = \left[\frac{g^2}{4} - \left(x - \frac{g}{2} \right)^2 \right]. \tag{2}$$

Substituting u(x) from Eq. (2) into Eq. (1), we obtain:

$$\left[\frac{\beta}{g} \right]^3 - \frac{3}{2} \left[\frac{\beta}{g} \right]^2 + \varepsilon \frac{1}{2} = 0. \tag{3}$$

This is the main equation governing the ideal DLD device and can be used to calculate D_c for the ideal DLD (Inglis et al. 2006). The non-parabolic flow profile or non-ideal boundary conditions (e.g. finite width and length of device) make Eq. (3) inaccurate (Inglis 2007). Thus the best way to predict the operation of DLD is to calculate particle trajectory in the whole channel.

2.2 EPTSM algorithm

A DLD device was designed based on the discussion above. In this design, we purposely chose a large gap distance in order to simplify the manufacturing process and to lower the probability of clogging (Inglis 2009; Zhu et al. 2010; Yan et al. 2015). Additionally, employing such a design yields higher device throughput and exerts lower shear stress on the particles. However, if the gap increases, in order to acquire the same lateral displacement for the larger particles, a longer channel is required.

The second step is to calculate the fluid parameters of the device using finite element method (FEM). No-slip boundary condition is assumed for walls and pillars interfaces. By solving Navier–Stokes equations, pressure and velocity field in the domain can be obtained. Then the fluid velocities in both x and y directions at all of mesh nodes are exported from this simulation.

In the third step these data were used in order to simulate the particle paths by proposed algorithm throughout the channel. Since the particles are only impacted by the surrounding fluid in each time step (dt), only meshes around the particle were considered in order to minimize the simulation runtime. Furthermore, time steps were reduced by one order of magnitude when particles approached walls or pillars to increase accuracy. The algorithm continues to calculate the particle coordinates and trajectories until they enter forbidden areas like inside the pillars or go beyond the channel boundaries. According to EPTSM, two corrections are performed on a particle under such circumstances; first the particle is moved backward along its streamline so that it would not be inside the pillar and its exterior surface only infinitesimally touch the pillar or wall. Second, we assumed that the particle velocity component toward inside of the pillar is damped to zero upon collision, and hence its normal velocity is set to zero so the particle would only have tangential velocity. After these two corrections, particle coordinates are recalculated. Figure 2 illustrates a simplified flowchart explaining the EPTSM by which particle trajectories were numerically evaluated.

The Re number in the channel of the DLD device is low, so that the fluid flow is in creeping regime and the inertial effects can be neglected. Moreover, as stokes number is in the order of 10^{-5}, we can assume that particle's velocity in each position is exactly the fluid velocity in the absence of the particles. Additionally, it is assumed that particles have no effect on the velocity profile of fluid flow.

Fig. 2 The EPTSM process
flowchart. Wall in the
figure refers to pillar or channel
boundaries

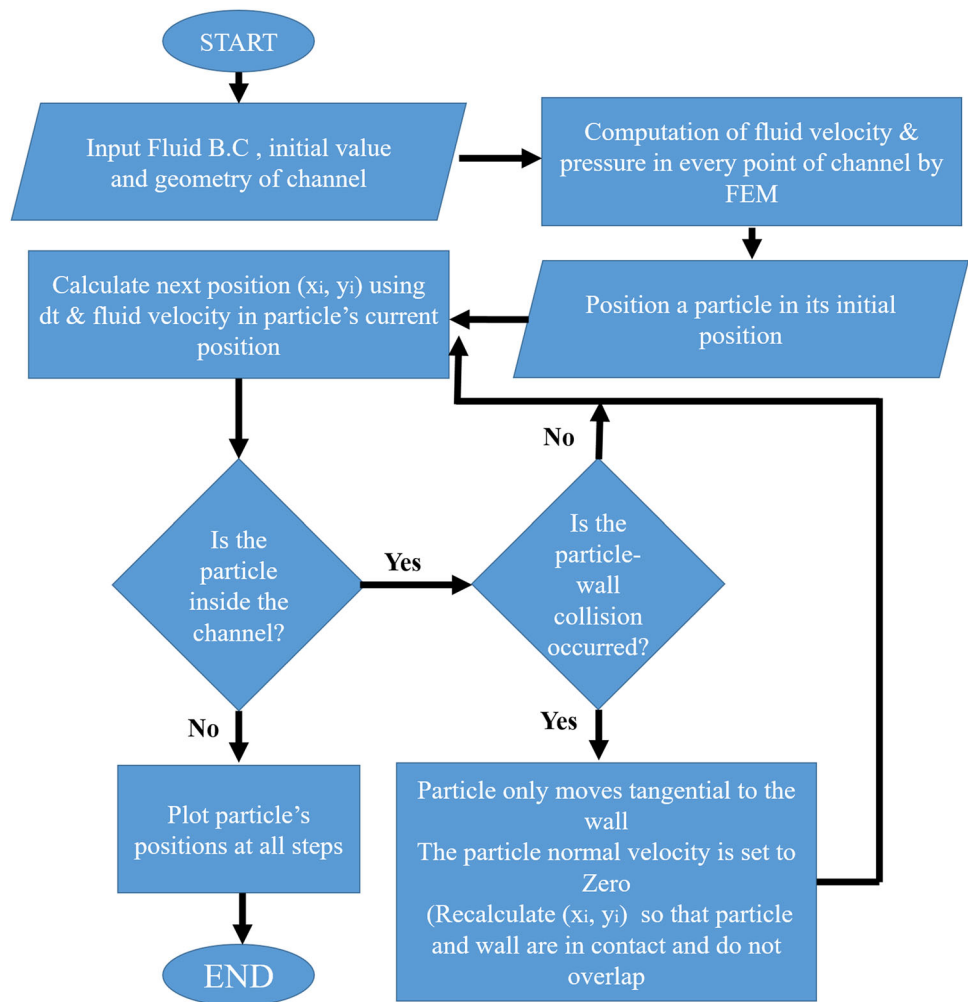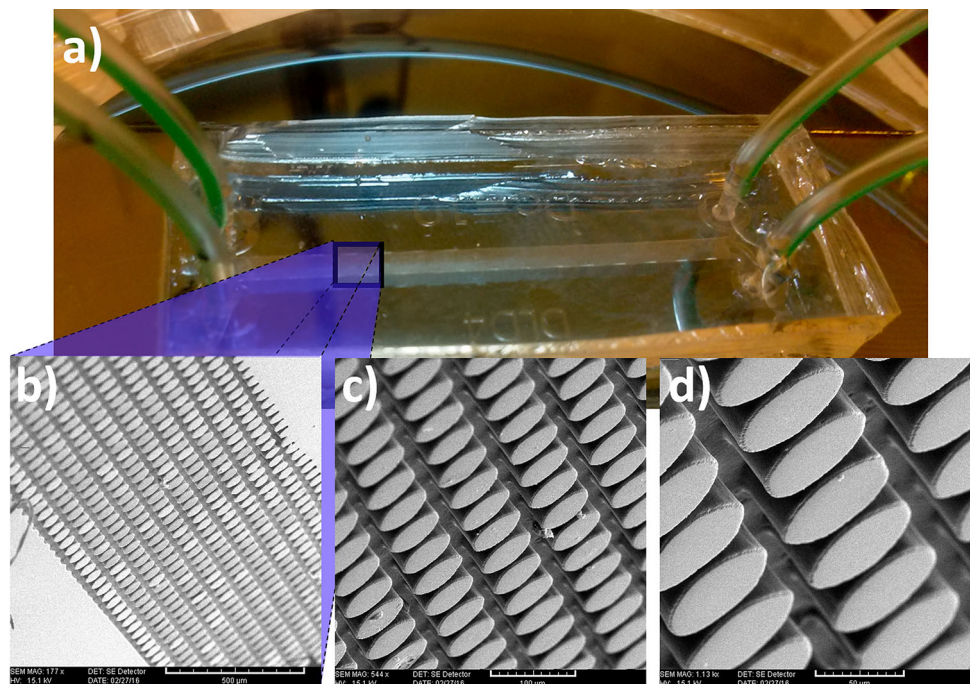**Fig. 3 a** A picture of the
fabricated device. **b–d** Scanning
electron micrographs of the
pillars in the main channel with
magnification in c and d, for
better clarity

2.3 Experiment

Figure 3 depicts a picture of the DLD device used in our experiment. The device consists of two inlets (for sample and buffer), two outlets, and one channel.

The devices were microfabricated using standard soft lithography techniques (Duffy et al. 1998). A 40-µm thick mold was fabricated by SU-8 2050 (MicroChem, Newton, MA, USA) on a silicone substrate. The channel was made by casting polydimethylsiloxane (PDMS, Sylgard 184, Dow Corning, USA) on the mold. PDMS monomer and curing agent were mixed to a ratio of 10:1. Plasma bonding was used to seal glass to PDMS. The DLD device was designed assuming $D_c = 5$ µm and employing (3). The pillars are cylinders, made of PDMS, with 50 µm diameter and size of the gaps between adjacent pillars are 40 µm. The width and the length of channel are 1 mm and 1 cm, respectively. Phosphate buffer saline (PBS) was used as the carrier fluid in the channel. The inlet flows for both sample and buffer was 4.5 µL/min.

3 Results and discussion

The magnitude of fluid velocity is calculated using numerical simulation and is shown in Fig. 4. The collision between the particles and the pillars has a dominant role in the DLD operation, thus calculating particle trajectory near the pillars is of critical importance in this device. As shown in Fig. 4, in order to achieve higher precision, the mesh elements near the pillars need to be smaller than g/2 and much less than D_c.

As mentioned earlier, the theory of the DLD is based on Poiseuille flow with parabolic velocity profile. However, since pillar's diameter is comparable with minimum gap size between pillars in the present DLD device, the flow profile deviates from parabolic shape (Inglis 2007). The horizontal component of fluid velocity between pillars across the channel and the fluid velocity profile predicted by Poiseuille flow under this condition is shown in Fig. 4c. According to (2), the critical diameter is related to the integral of flow profile. Thus it is expected that the calculated D_c be smaller than the designed D_c.

Finally, the particle trajectory must be calculated. For this purpose, results of velocity profile simulation are used to calculate the particle velocity in each time step by EPTSM method as elaborated earlier. First, an initial position and velocity is assumed for the particle. The position of the particle in the next step is calculated assuming constant velocity for particle. Then, the velocity of the particle is calculated by interpolating between fluid velocities in the nearest three mesh points. The velocity of any particle inside the mesh triangle is proportional to the distance of particle to triangle nodes. The independence of the particle trajectory and mesh size was verified by using different mesh sizes and checking if the particle trajectory remains the same when a finer mesh is used. Furthermore, in the utilized mesh, the fluid velocity profile is smoothed and kept invariable when mesh size is decreased.
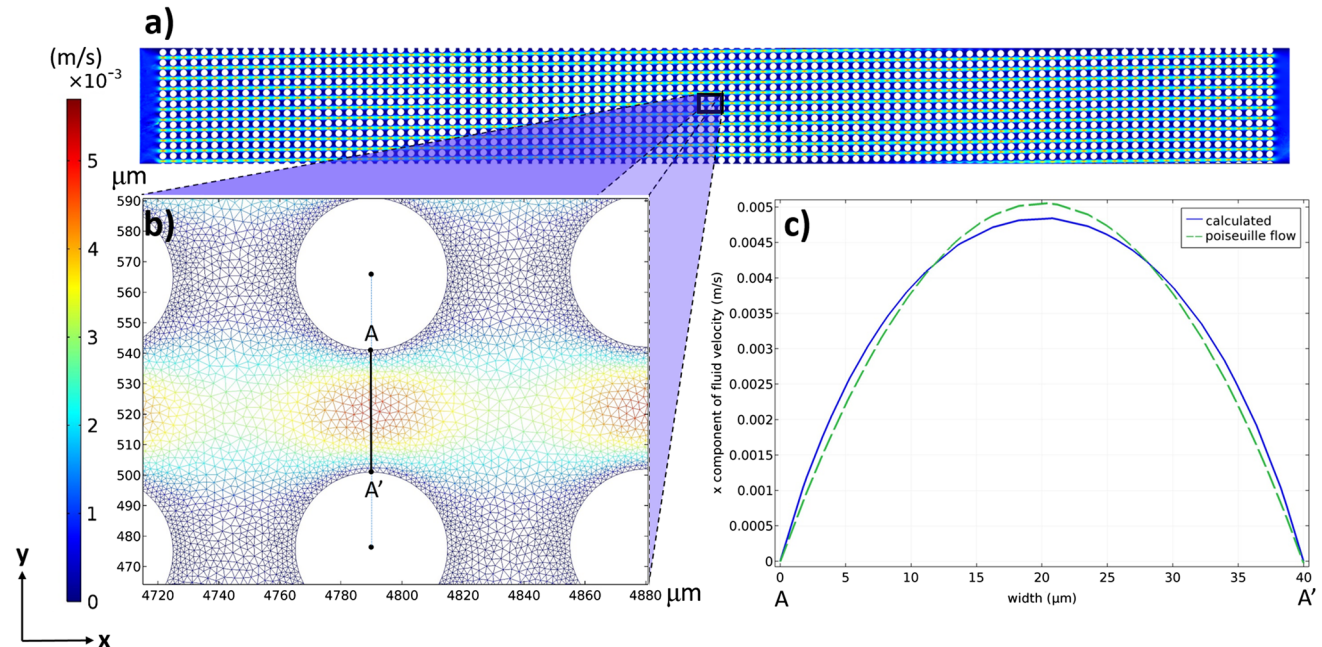

Fig. 4 Fluid velocity magnitude in the DLD device: **a** a bird's eye view of the device, **b** velocity magnitude and mesh size between pillars. **c** Component of fluid velocity along the x direction between pillars (A–A′ line) and the fluid velocity profile as predicted by Poiseuille flow

Additionally, the time step to calculate the particle trajectory is 10^{-5} s. This value depends on the average fluid velocity in the channel. The particle trajectory computed with the above mentioned time step is exactly the same as particle path utilizing time step equal to 10^{-6} s. As a consequence, these results also verify independency of particle time step from its trajectory

The numerical simulation in Fig. 5 depicts how the particle trajectories for the 4 μm and 6 μm particles, shown by the blue and magenta colored circles, respectively, deviate inside the channel. In Fig. 5, particle positions are depicted with 2 ms time step to distinguish the particles velocity in different intervals. In this way, center-to-center distance of a particle in consecutive time steps, shows the changes in velocity. As expected, larger particle follows the bump mode and smaller one follows the zigzag mode. These simulation results show that this device can separate particles with diameters 4 μm and 6 μm. By considering that the critical diameter for the device is assumed to be 5 μm, it can be concluded that the DLD theory verifies this simulation, and this simulation is able to predict the correct particle trajectory in the DLD.

To confirm these results a DLD device was accordingly designed and fabricated. The pillar diameter, the gap size and the height of the channel were 65, 25 and 50 μm,

respectively and ε was 1/90. By substituting these parameters in (3), we find that $D_c = 3.1$ μm. The device was tested with various sizes of Polystyrenes particles (between 1 and 15 μm). The average velocity of the fluid in the channel was set to 3 μL/min. Particle trajectory images are produced with overlaying multiple optical microscope images in sequences of the time steps. The trajectories of the 3 and 6.2 μm PS particles are shown in Fig. 6a, b. The time step between frames is 1/30 s, thus the particle displacement in each frame is proportional to the particle velocity. The same experimental parameters, including geometrical parameters, particle size, inlet velocity of the fluid and the particles releasing points, were used to simulate the device with EPTSM in above. The results of the simulation are shown in Fig. 6c, d. As shown in Fig. 6 the particles path line predicted by simulation, exactly matches the one obtained by experiment in both zigzag and bump modes. Thus the simulation results clearly verify experimental outcomes.

Finally, we have numerically examined how the trajectory of the RBCs deviates from that of WBCs throughout the channel. In this simulation, RBC is assumed to be spherical with a diameter equal to 2.5 μm while WBC were assumed 10 μm diameter spheres. The trajectory for 11 RBCs and 11 WBCs is calculated by EPTSM. A picture of
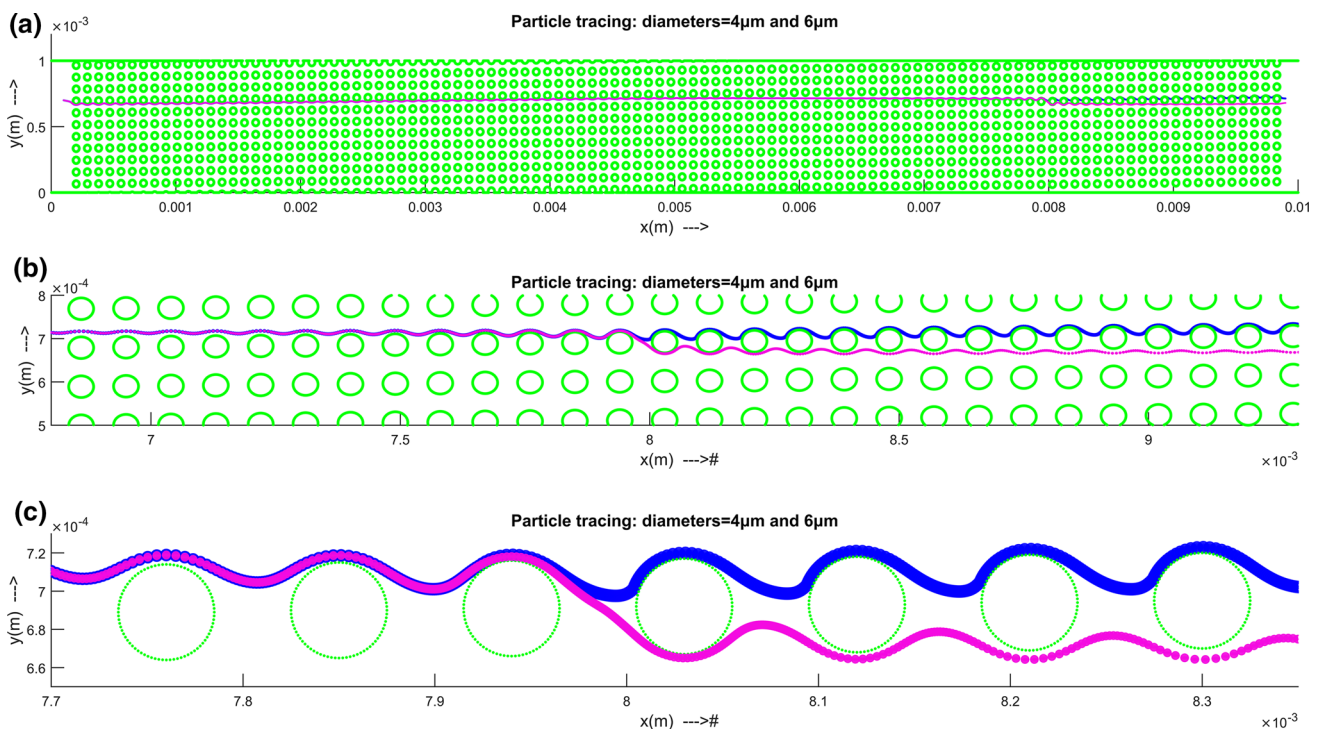

Fig. 5 Deviation of the particle trajectories having sizes 4 μm and 6 μm by the DLD device with $D_c = 5$ μm in the channel. Six micron particle (blue circle) traverses the channel in the bump mode and moves towards the upper channel wall while the 4 μm size particle (magenta circle) traverses the channel in a zigzag mode with a net lateral displacement of approximately zero. **a** A bird's eye view showing trajectories through the channel. **b** Anomaly of particles' trajectories with different sizes. **c** Velocity changes of a particle is deduced by tracking center-to-center distance of particle positions in the consequent time steps (color figure online)

Fig. 6 Verification of the simulation results with experimental outcomes: the experimental trajectory of **a** 3 μm particle and **b** 6.2 μm particle. The simulated trajectory of **c** the 3 μm particle and **d** the 6.2 μm particle (pictures were generated by overlaying of multiple video frames)
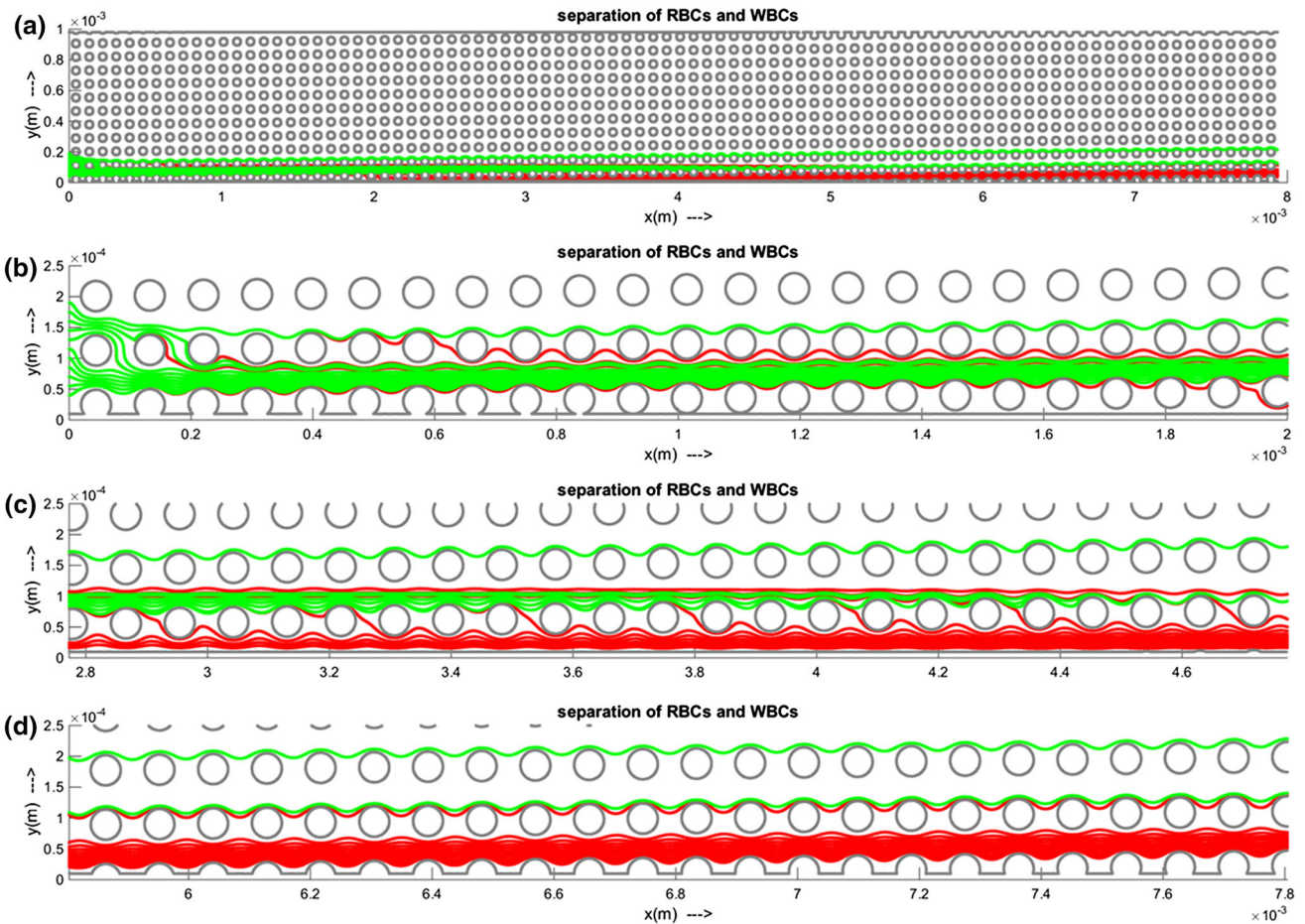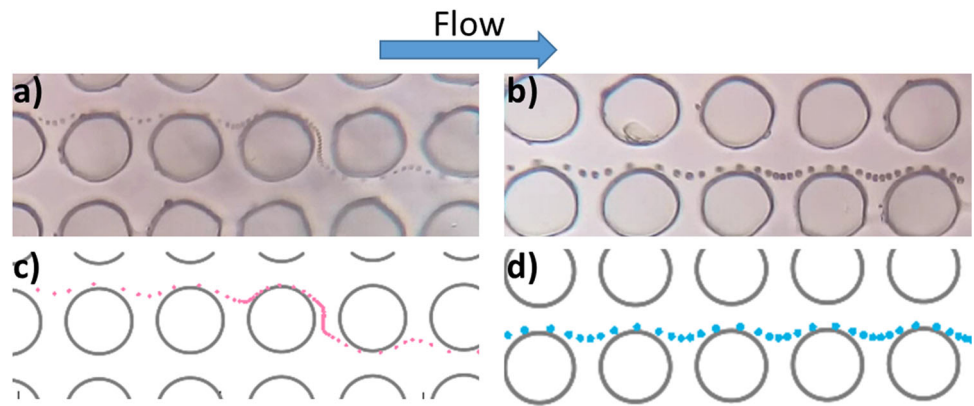

Fig. 7 Results of numerical calculations of the trajectories for 11 RBCs (red) and 11 WBCs (green) using our proposed method. Deviation of the trajectories **a** throughout the entire channel.

b Section at the beginning of the channel. **c** Section at the middle of the channel. **d** Section at the end part of the channel (color figure online)

the entire device is shown in Fig. 7 showing trajectories for all particles, assuming the same initial positions. Figure 7a shows the results throughout the entire channel. Furthermore, Fig. 7b–d depict an enlarged view for the beginning section, middle section and the end part of the channel respectively, illustrating how the particles separate once

they approach the end of the channel. At the middle of the channel (Fig. 7c) the separation is not completed. As seen RBCs and WBCs are separated near the end of the channel (Fig. 7d). As the behavior of particles are similar around all pillars, the resulting lateral displacement can be amplified elongating channel length to the point that heterogeneous

Table 1 Comparison of proposed EPTSM with previous works

Method	Accuracy	Simulated channel size	Approximate run time	References
Lattice–Boltzmann	Verified with theory (not experimental verification)	$32 \times 32 \times 4.8$ μm	Proportional to Re^{-1}	Krüger et al. (2014)
Automatic dynamic incremental nonlinear analysis	Verified with theory (no experimental verification)	1000×1500 μm	> 5 h	Khodaee et al. (2016)
COMSOL-MATLAB	Verified with theory (no experimental verification)	130×300 μm	> 2 h	Al-Fandi et al. (2011)
The EPTSM (proposed method)	Verified with experiment	$10{,}000 \times 1000$ μm (total channel size)	0.5 h	This work

particles are divided enough so that when they reach a bifurcation at the end of the channel, samples received at each outlet would be appropriately separated.

In Krüger et al. (2014), Lattice and Boltzmann provided a method for predicting particle's trajectory by solving fluid equations with particle motion equation in each time step. However, in EPTSM, the interactions between fluid and particle are neglected, so the fluid equations are solved only once, this enhances convergence rate comparing to the one proposed in Krüger et al. (2014). Furthermore, present method demonstrates remarkable accuracy as verified by our experimental results without any need for unjustified assumptions (e.g. periodic boundary condition).

Results of our EPTSM for accuracy, the size of simulated portion of the channel and the run time are compared with previous methods' by repeating and converging the mentioned works on one computer. These results are tabulated in Table 1.

4 Conclusion

In this work, the EPTSM algorithm was introduced for the numerical simulation of the particle trajectories in microfluidics devices. Although the method is general, its capabilities was demonstrated only for a DLD device. The method uses FEM to solve fluid equations, then the results are used for particle tracing in the channel. This method provides an efficient procedure for finding particle trajectories in many non-inertial microfluidics devices in which particle size and its collisions with walls of the channel cannot be neglected. Hence, the functionality of the device can be estimated prior to manufacturing. The short execution time of this method enables identification of the trajectories of several particles through the channel. Although this model is used to predict the behavior of the non-inertial microfluidics devices, it can be modified for use in other kinds of devices, such as pinched flow fractionation (PFF) devices (Takagi et al. 2005). Furthermore, the method is expected to be particularly efficient in the prediction of the trajectories in 3D microfluidic geometries as well as the large systems and allows for taking into account extra particle parameters such as particle deformability within a reasonable simulation run time.

References

Al-Fandi M et al (2011) New design for the separation of microorganisms using microfluidic deterministic lateral displacement. Robot Comput Integr Manuf 27(2):237–244

Balvin M et al (2009) Directional locking and the role of irreversible interactions in deterministic hydrodynamics separations in microfluidic devices. Phys Rev Lett 103(7):078301

Beech J (2005) Deterministic lateral displacement devices. MSc, Lund University

Beech J (2011) Microfluidics separation and analysis of biological particles. Fasta Tillståndets Fysik

Beech JP, Jönsson P, Tegenfeldt JO (2009) Tipping the balance of deterministic lateral displacement devices using dielectrophoresis. Lab Chip 9(18):2698–2706

Çetin B, Li D (2011) Dielectrophoresis in microfluidics technology. Electrophoresis 32(18):2410–2427

Chen Y et al (2014) Rare cell isolation and analysis in microfluidics. Lab Chip 14(4):626–645

Choi S et al (2014) High-throughput DNA separation in nanofilter arrays. Electrophoresis 35(15):2068–2077

Davis JA et al (2006) Deterministic hydrodynamics: taking blood apart. Proc Natl Acad Sci 103(40):14779–14784

Duffy DC et al (1998) Rapid prototyping of microfluidic systems in poly (dimethylsiloxane). Anal Chem 70(23):4974–4984

Green JV, Radisic M, Murthy SK (2009) Deterministic lateral displacement as a means to enrich large cells for tissue engineering. Anal Chem 81(21):9178–9182

Huang LR et al (2004) Continuous particle separation through deterministic lateral displacement. Science 304(5673):987–990

Hyun KA, Jung HI (2013) Microfluidic devices for the isolation of circulating rare cells: a focus on affinity-based, dielectrophoresis, and hydrophoresis. Electrophoresis 34(7):1028–1041

Inglis D (2007) Microfluidic devices for cell separation. Princeton University, Princeton

Inglis DW (2009) Efficient microfluidic particle separation arrays. Appl Phys Lett 94(1):013510

Inglis DW et al (2006) Critical particle size for fractionation by deterministic lateral displacement. Lab Chip 6(5):655–658

Inglis DW et al (2008) Microfluidic device for label-free measurement of platelet activation. Lab Chip 8(6):925–931

Jin C et al (2014) Technologies for label-free separation of circulating tumor cells: from historical foundations to recent developments. Lab Chip 14(1):32–44

Khodaee F et al (2016) Numerical simulation of separation of circulating tumor cells from blood stream in deterministic lateral displacement (dld) microfluidic channel. J Mech 32(4):463–471

Krishnan JN et al (2009) Rapid microfluidic separation of magnetic beads through dielectrophoresis and magnetophoresis. Electrophoresis 30(9):1457–1463

Krüger T, Holmes D, Coveney PV (2014) Deformability-based red blood cell separation in deterministic lateral displacement devices—a simulation study. Biomicrofluidics 8(5):054114

McGrath J, Jimenez M, Bridle H (2014) Deterministic lateral displacement for particle separation: a review. Lab Chip 14(21):4139–4158

Quek R, Le DV, Chiam K-H (2011) Separation of deformable particles in deterministic lateral displacement devices. Phys Rev E 83(5):056301

Smith JP et al (2012) Microfluidic transport in microdevices for rare cell capture. Electrophoresis 33(21):3133–3142

Takagi J et al (2005) Continuous particle separation in a microchannel having asymmetrically arranged multiple branches. Lab Chip 5(7):778–784

Vig AL (2010) Pinched flow fractionation—technology and application. Ph.D. thesis, Department of Micro-and Nanotechnology Technical University of Denmark

Yan S et al (2015) A hybrid dielectrophoretic and hydrophoretic microchip for particle sorting using integrated prefocusing and sorting steps. Electrophoresis 36(2):284–291

Zheng S et al (2005) Deterministic lateral displacement MEMS device for continuous blood cell separation. In: Micro electro mechanical systems, 2005. MEMS 2005. 18th IEEE international conference on, IEEE

Zhu J, Tzeng TRJ, Xuan X (2010) Continuous dielectrophoretic separation of particles in a spiral microchannel. Electrophoresis 31(8):1382–1388